

# CORRECTION TECHNOLOGY FOR MAIN GIRDER TORSION IN A COMPOSITE GIRDER CABLE-STAYED BRIDGE

She, Q. C.<sup>\*,\*\*</sup>; Yan, D. H.<sup>\*</sup>; Chen, C. S.<sup>\*#</sup>; Li, B.<sup>\*\*</sup> & Huang, G.<sup>\*</sup>

<sup>\*</sup> School of Civil Engineering, Changsha University of Science and Technology, 410114, Changsha, China

<sup>\*\*</sup> College of Civil Engineering and Architecture, Hunan Institute of Science and Technology, 414006, Yueyang, China

E-Mail: changsongchen@csust.edu.cn (# Corresponding author)

## Abstract

To solve the problem of the steel longitudinal beam being unable to match precise installation of the steel main beam due to torsional deformation during the steel installation process of a composite twin-box girder cable-stayed bridge, a torsion correction method through the multipoint jacking adjustment of transverse steel beams is proposed. Based on the constrained torsion calculation theory for closed thin-walled members, a constrained torsion differential equation for steel longitudinal beams and its general solution were established. Then, the torsion angle and the jacking force on each steel beam at zero torsion angles were obtained. In addition, a local refined model by the finite element software Abaqus was established, simulating the jacking process with the transverse steel beams as a lever arm. The accuracy of the theoretical and numerical analysis was verified by the measured results on site. Results show that the torsion angle of the steel longitudinal beam could be adjusted through multipoint jacking of the steel crossbeam, the installation error caused by the torsion is effectively eliminated, and the efficiency and accuracy of the composite twin-box girder cable-stayed bridge are improved. (Received in April 2023, accepted in July 2023. This paper was with the authors 1 month for 1 revision.)

**Key words:** Composite Girder Cable-Stayed Bridge, Main Girder Torsion, Finite Element Analysis, Correction Technology

## 1. INTRODUCTION

A composite girder is a form of a main girder in which the concrete bridge deck and the steel beams are assembled through shear connectors. Compared with the concrete main girder, the composite girder is more suitable for long-span cable-stayed bridges owing to its lighter dead weight and easier-to-control construction quality. Compared with the high-cost and complexly stressed orthotropic steel bridge deck of the steel box girder, the concrete bridge deck of the composite girder has lower cost and higher rigidity. Therefore, steel-concrete composite girders are widely applied in cable-stayed bridges with a main span of 400–700 m because of their light weight, high structural rigidity and excellent dynamic performance [1, 2]. However, during the double-cantilever construction of the main girder of the composite girder cable-stayed bridge, manufacturing and installation errors often cause deformation and torsion of the main girder after the installation of a section of the main girder, making the subsequent section difficult to assemble and connect, thereby affecting the construction progress [3].

In view of this, scholars studied the deformation and torsion of the main girders of cable-stayed bridges with different structural types during the cantilever assembly [4-6]. However, the main girder of the composite girder cable-stayed bridge has undergone multiple system transformations during the construction stage. In addition, the deformation and torsion angle of the main girder changes with different construction conditions because of the complex stress of the main girder and the unstable structural system in the double-cantilever construction stage. Therefore, accurately assessing the deformation and torsion effects of the

main girder of the composite girder cable-stayed bridge and finding an efficient method to correct the deformation and torsion are urgent problems to be solved.

Thus, this study establishes a constrained torsion calculation theory for closed thin-walled members based on theoretical calculations, finite element models and field measurements and obtains the torsion angle. The simulated results are compared with those of the ABAQUS finite element model and those measured at the construction site. The objectives are to create accurate measures to correct the torsion of the main girder during the construction stage and to provide a reference for the construction of composite twin-box girder cable-stayed bridges.

## **2. STATE OF THE ART**

Scholars conducted considerable work on the main girder of composite girder cable-stayed bridges. Cai et al. [7] used the finite element method (FEM) to study the vertical deformation and bridge deck stress of the to-be-installed girder section and the installed cantilever girder section of the Navigation Opening Bridge of Taizhou Bay Sea-Crossing Bridge under the construction stage loads. The objective is to ensure the accurate connection of the composite steel box girders of cable-stayed bridges during cantilever construction. Cai et al. also analysed the influence of the length of the hoisting segment, the position of the crane and the forced alignment measures on the vertical deformation of the section and the bridge deck stress. They found that adjusting the lateral position of the bridge deck crane can reduce the relative vertical deformation difference of the alignment section. However, the adjustment period is long and affects the safety of the structure. From another aspect, Jiang and Tang [8] used the finite element software Abaqus to establish a segment model. They also analysed the effect of lateral spacing of the bridge deck cranes on the deformation of installed and hoisting girder sections, including the lateral anti-overturning stability and relative misalignment of the hoisting girder section. The objectives are to solve the problem of large local deformation caused by the hoisting girder section of the bridge deck crane during the construction of the main girder of the bridge and realise the accurate alignment and installation of the girder section. Their results indicate that the girder segments can be precisely aligned by welding the side web first and then partially loosening the hook of the bridge deck crane. However, the measure will generate a large additional torsion on the web. The main girder erection schemes for composite girder cable-stayed bridges generally adopt one cycle per segment; that is, after the installation of the steel main girder and the bridge deck, the tensioning of the stay cables and the pouring and curing of the wet joints are carried out [9-12]. The advantage of 'one cycle per segment' is that this case can greatly control the internal force of the main girder but requires considerable cable tensioning, wet joint pouring cycles and a long construction period, particularly when the main girder is in the large cantilever construction stage for a long time. Wang et al. [13, 14] carried out systematic in situ stress monitoring of the composite girder of a twin I-shaped composite steel girder cable-stayed bridge under constant load. They also collected the normal stress data of the main girder of the bridge during construction and operation. Furthermore, they established a finite element model for numerical simulation and indoor segmental model testing and analysed the variation pattern of the shear lag effect. Wang et al. concluded that cable spacing and bridge deck are the main factors affecting the shear lag effect under constant loads. She et al. [15] built a full model and a local spatial model of a composite girder cable-stayed bridge by combining the finite element (FE) and field measurement methods to analyse the shear-lag effect in the composite twin-box girder under multiple typical construction conditions through numerical simulation and comparison with field measurements. Meanwhile, Zhao et al. [16] established a refined model of a lightweight composite twin-box girder by using finite element software to achieve accurate alignment of girder segments. They also simulated the whole process of main girder

hoisting and cable tensioning and proposed an external prestress-graded tensioning-girder replacement integrated light-weight twin-box composite girder correction technology system. This system has effectively reduced the deformation difference between the new and old sections of the main girder and improved assembly accuracy. Then, Atmaca and Atos [17] conducted a nonlinear static study on the structural behaviour of the bridge, including the shrinkage and creep of the concrete and the sag of the stay cables, by establishing a spatial finite element model of a composite girder cable-stayed bridge. They found that the construction scheme has a great influence on the structural behaviour of the bridge. Based on a simple linear girder model and parametric analysis, Giaccu et al. [18] proposed a method for calculating deck stresses in composite girder cable-stayed bridges. This method can help identify the actual detailed stress trends in concrete slabs and steel beams of the composite girder and is suitable for composite girder cable-stayed bridges with different geometric shapes. Szurgott and Bernacki [19] researched steel-concrete bridges under the action of high-speed trains. The results are plotted as a function of train velocity, thus permitting an assessment of the dynamic response of the bridge for each span length. Based on the principle of fatigue damage, Gao et al. [20] analysed the fatigue failure morphology and crack development of the test composite girder under equivalent fatigue load.

Gara et al. [21, 22] incorporated four displacement functions into the virtual work equation and solved the numerical equations via the FEM to analyse the shear lag and slip effects of composite girders. However, the results had certain errors because of spatial discretisation.

The above studies mainly focused on the analysis of the reasons for the deformation and torsion and the spatial force behaviour of the main girders of composite girder cable-stayed bridges of different structural types during the cantilever construction stage of the main girder through finite element numerical simulation. However, studies on the deformation and torsion of the main girder in the construction stage of composite twin-box girder cable-stayed bridges are limited. Moreover, studies on technologies that correct the main girder torsion through theoretical analysis and calculation are scarce. Hence, this study analyses the deformation and torsion of the main girder of a composite girder cable-stayed bridge through theoretical calculation, numerical simulation and field measurements. The study also proposes a torsion correction method through multipoint jacking adjustment of steel transverse beams, providing a basis for the construction of the main girders of composite twin-box girder cable-stayed bridges. The objectives are to develop the correction technology for the deformation and torsion of the main girder in the main girder erection stage of composite twin-box girder cable-stayed bridges and ensure the smooth progress of the main girder erection.

The rest of this paper is organized as follows. Section 3 establishes the restraint torsion differential equation for steel longitudinal beams. This section also solves the general solution of the differential equation through the initial parameter method based on the sector geometry characteristics of the steel longitudinal beam section. In addition, this section derives a theoretical calculation formula for the jacking forces in the jacking adjustment of transverse steel beams, establishes a local model using Abaqus and numerically analyses the jacking adjustment. Then, Section 4 verifies that the theoretical analysis and modelling methods have good accuracy by comparatively analysing the data obtained from the theoretical analysis, the finite element calculation model and the field measurement. Finally, Section 5 summarises the paper with relevant conclusions.

### **3. METHODOLOGY**

The construction of the steel main girder of the composite twin-box girder cable-stayed bridge generally adopts segmental assembly. Specifically, the steel longitudinal beams on both sides

are installed first. Then, the steel transverse beams are installed at the cantilever front end of the main girder, and finally, the small longitudinal beams are installed to form a frame system (Fig. 1). However, after the steel longitudinal beams on both sides are installed, installation errors generally occur, and such errors will cause internal torsion of the cross-section. This case results in a vertical height difference between the top plates of the steel transverse beams and the top plate of the steel longitudinal beams and a vertical height difference between the inner and outer sides of the top plate of the steel longitudinal beams. Consequently, this case will lead to the failure to connect the steel transverse beams and the steel longitudinal beams through splice plates. As shown in Fig. 1, assume that the torsion angles of the left and right steel longitudinal beams are  $\theta_1$  and  $\theta_2$ , respectively. In this case, if the steel transverse beams are first spliced with the left steel longitudinal beam, then a vertical height difference  $\delta_v(\theta_1 L)$  will exist between the right side of the top plates of the steel transverse beams and the top plate of right steel longitudinal beam. This height difference will result in a misalignment between the bolt holes of the steel longitudinal and transverse beams and those of the splice plates (Fig. 2).

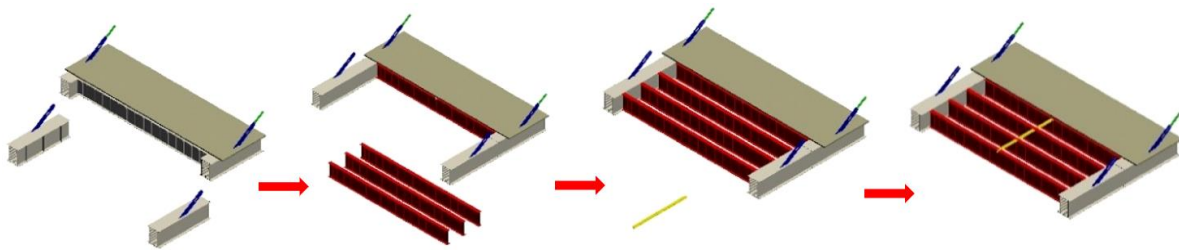


Figure 1: Installation sequence of the steel main girder.

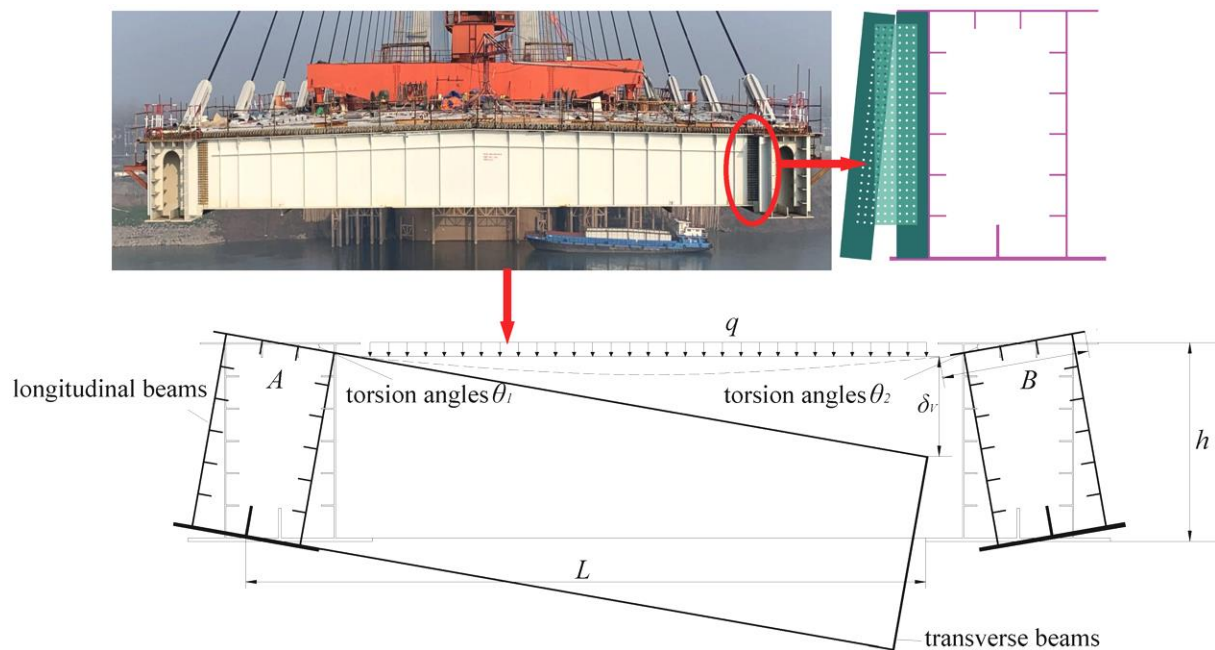


Figure 2: Rigid torsion of the steel longitudinal beam cross-section caused by installation errors.

### 3.1 Theoretical analysis

**The solution of the constrained torsion differential equation:** Considering that the cantilevers of the top and bottom plates of the steel longitudinal beams are very short, their contribution to the torsion resistance of the main girder is limited. Therefore, their contribution is ignored in the following theoretical analysis. Fig. 3 shows the torsion equivalent calculation diagram of the steel longitudinal beams.

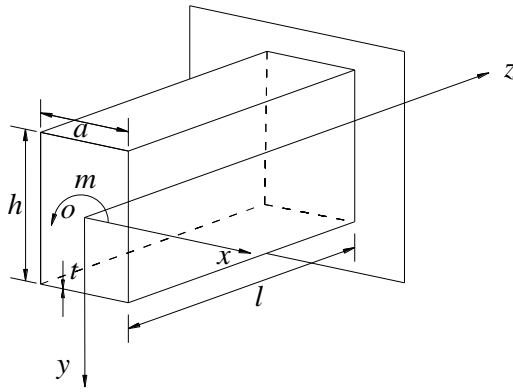


Figure 3: The torsion equivalent calculation diagram of the steel longitudinal beams.

The constrained torsion differential equation for closed thin-walled members is used:

$$M_z = M_f + M_w$$

where  $M_z$  is the total torque of the member section,  $M_f = GJ\varphi'$  is the free torque,  $M_w = -EI_w\theta_\omega''$  is the secondary torque,  $\varphi$  is the angle of free torsion,  $\theta_\omega$  is the warping function,  $J$  and  $I_w$  are the torsional and sectoral moment of inertia of the section, respectively and  $G$  and  $E$  are the shear modulus and elastic modulus, respectively. The constrained torsion differential equations for steel longitudinal beams are obtained as follows:

$$\frac{1}{\mu} EI_\omega \varphi^{IV} - GJ\varphi'' = -m$$

According to the sector geometry characteristics of the steel longitudinal beam section, the following can be obtained:

$$\mu = 1 - \frac{J}{I_p} = 1 - \frac{4ah}{(a+h)^2}$$

where  $J$  is the torsional moment of inertia of the section.  $J = \frac{4\hat{A}^2}{\oint \frac{ds}{t}} = \frac{4(ah)^2}{2\left(\frac{a+h}{t}\right)}$ , where  $\hat{A}$  is

the area surrounded by the centreline of the thin wall of the section.  $I_p$  is the polar moment of inertia of the section relative to the torsion centre.  $I_p = \oint r^2 ds = \frac{ah(a+h)t}{2}$ .

The constrained torsion differential equation for steel longitudinal beams is established based on the constrained torsion calculation theory for closed thin-walled members. In addition, the general solution of the differential equation is solved through the initial parameter method based on the sector geometry characteristics of steel longitudinal beams. The torsion angle  $\varphi$  can be obtained as follows:

$$\varphi = \frac{m}{kGJ} \left[ k(z-l) - \frac{\mu shkz}{chkl} + \mu thkl \right]$$

In the formula, the coefficient  $k = \sqrt{\mu \frac{GJ}{EI_\omega}}$ .  $I_\omega = \oint \omega^2 t ds = \frac{a^2 h^2 (h-a)^2 t}{24(a+h)}$ , where  $\omega$  is the

sector coordinate of the section.

**Solution of the jacking force:** Considering the long length of the steel transverse beams, the jacking force provided by the jack will generate a large moment of a couple for the steel longitudinal beams. An appropriate multipoint jacking of steel transverse beams can correct the torsion, aligning the bolt holes of the longitudinal and transverse beams with those of the splice plates. To this end, this study proposes a torsion correction method through multipoint jacking adjustment of steel transverse beams, as shown in Fig. 4.

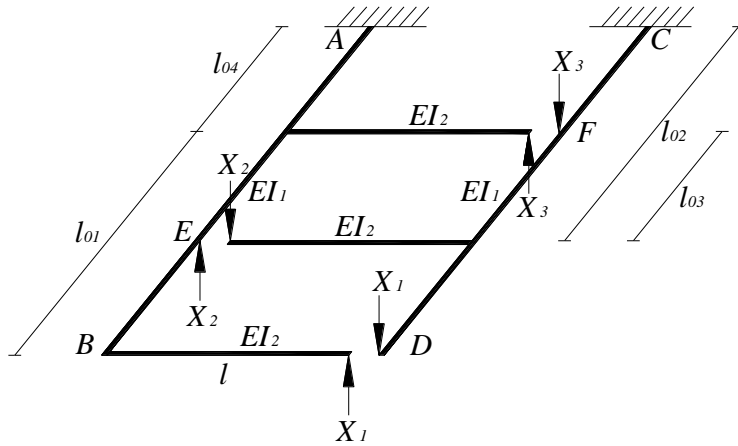


Figure 4: Simple calculation diagram of multipoint jacking adjustment of transverse beams.

Denoting the jacking force on steel transverse beam 3 at D as  $X_1$ , the torsion angle of the left longitudinal beam AB is as follows:

$$\varphi_1(z) = \frac{X_1 l}{kGJ} \left[ k(z-l_0) - \frac{\mu shkz}{chkl_0} + \mu thkl_0 \right] \quad (1)$$

Hence, transverse beam 1 rotates in the XY plane by  $\varphi_1(l_{01})$ .

Next, denoting the jacking force on steel transverse beam 2 at E as  $X_2$ , the torsion angle of the right longitudinal beam CD is as follows:

$$\varphi_2(z) = \frac{X_2 l}{kGJ} \left[ k(z-l_{02}) - \frac{\mu shkz}{chkl_{02}} + \mu thkl_{02} \right] \quad (2)$$

To make the right longitudinal beam horizontal in the XY plane at point F, the torsion angle of the right longitudinal beam at point F is as follows:

$$\varphi_2(l_{03}) = \theta_2 - \frac{X_3 l^2}{2EI_2} \quad (3)$$

Finally, denoting the jacking force on steel transverse beam 1 at F as  $X_3$ , the torsion angle of the left longitudinal beam AB is as follows:

$$\varphi_3(z) = \frac{X_3 l}{kGJ} \left[ k(z-l_{04}) - \frac{\mu shkz}{chkl_{04}} + \mu thkl_{04} \right] \quad (4)$$

Therefore, transverse beam 1 rotates in the XY plane by  $\varphi_3(0)$ . To make the left longitudinal beam horizontal in the XY plane at F point,

$$\varphi_1(l_{01}) + \varphi_3(0) = \theta_1 \quad (5)$$

Under the combined action of  $X_1$ ,  $X_2$  and  $X_3$ , the vertical displacement of transverse beam 1 at the free end F,  $v_{FL}$ , is as follows:

$$v_{FL} = \varphi_1(l_{01})l + \frac{X_1(l_0 - l_{01})^2}{6EI_1}(2l_0 + l_{01}) - \frac{X_2(l_{02} - l_{03})^2}{6EI_1}(2l_{02} + l_{03}) + \varphi_3(0)l + \frac{X_3 l_{04}^3}{3EI_1} + \frac{X_3 l^3}{3EI_2} \quad (6)$$

The vertical displacement of the right longitudinal beam at point F,  $v_{FR}$ , is as follows:

$$v_{FR} = \frac{X_1(l_0 - l_{01})^2}{6EI_1}(2l_0 + l_{01}) - \frac{X_2(l_{02} - l_{03})^2}{6EI_1}(2l_{02} + l_{03}) + \frac{X_3 l_{04}^3}{3EI_1} \quad (7)$$

To make the elevations of transverse beam 1 and the right longitudinal beam at point F the same,

$$v_{FL} + v_{FR} = \theta_1 l \quad (8)$$

The jacking forces  $X_1$ ,  $X_2$  and  $X_3$  can be obtained by combing Eqs. (3), (5) and (8).

$$X_1 = -\frac{-AF\theta_1 + BG\theta_1 + ADI\theta_1 - DG\theta_2}{-ADE + ACF - BCG} \quad (9)$$

$$X_2 = -\frac{-BE\theta_1 - BCI\theta_1 - DE\theta_2 + CF\theta_2}{ADE - ACF + BCG} \quad (10)$$

$$X_3 = -\frac{-AE\theta_1 + ACI\theta_1 - CG\theta_2}{-ADE - ACF + BCG} \quad (11)$$

where:  $A = \frac{l}{kGJ} \left[ k(l_{03} - l_{02}) - \frac{\mu shkl_{03}}{chkl_{02}} + \mu thkl_{02} \right]$ ;  $B = \frac{l^2}{2EI_2}$ ;

$$C = \frac{l}{kGJ} \left[ k(l_{01} - l_0) - \frac{\mu shkl_{01}}{chkl_0} + \mu thkl_0 \right]$$
;  $D = \frac{l}{kGJ} (-kl_{04} + \mu thkl_{04})$ ;

$$E = \frac{l^2}{kGJ} \left[ k(l_{01} - l_0) - \frac{\mu shkl_{01}}{chkl_0} + \mu thkl_0 \right] + \frac{X_1(l_0 - l_{01})^2}{3EI_1} (2l_0 + l_{01})$$
;

$$F = \frac{l^2}{kGJ} (-kl_{04} + \mu thkl_{04}) + \frac{2l_{04}^3}{3EI_1} + \frac{X_3 l^3}{3EI_2}$$
;  $G = -\frac{(l_{02} - l_{03})^2}{3EI_1} (2l_{02} + l_{03})$ .

### 3.2 Simulation analysis

Key issues such as selection, meshing, boundary conditions and interfaces in the establishment of the FEM using ABAQUS are briefly introduced as follows:

**Selection of element type and meshing:** Steel longitudinal beams and steel transverse beams are represented by three-dimensional eight-node brick elements with reduced integration (C3D8R). Meshing is performed through structured meshing technology whilst maintaining the consistency of the mesh of the contact part.

**Simulation of the cross-section:** Models of steel longitudinal beams and steel transverse beams are established, and then, a section of steel longitudinal beams and a section of steel beams are directly merged through the ‘merge’ function.

**Boundary conditions and load forms:** One end of the steel longitudinal beams is consolidated, and the other end is cantilevered, which is consistent with the actual situation of the project. The jacking forces  $X_1$ ,  $X_2$  and  $X_3$  are replaced by pressure.

This study chooses to solve in the ABAQUS/Standard module. The structural displacement at any position on the main girder can be obtained through local analysis, and the obtained data can be used for subsequent analysis. Fig. 5 shows the finite element models of local space.

## 4. RESULT ANALYSIS AND DISCUSSION

### 4.1 Project overview

One composite girder cable-stayed bridge is a steel-concrete composite beam cable-stayed bridge with two towers and two cable surfaces. The elevation arrangement is shown in Fig. 6 a. The span of the main bridge is arranged as (90 + 240 + 720 + 240 + 90) m, which main span is 720 m. The bridge floor width is 36.5 m, and the cross-section diagram is shown in Fig. 6 b. The main girder of the composite girder adopts the form of a twin-box section, and this is formed by connecting the box-shaped steel main girder and the precast concrete bridge deck through shear connectors arranged on the longitudinal beams, transverse beams, and small longitudinal beams. The length of the standard segmental steel main beam is 12 m and width is 35.12 m, consists by two side steel box beams, three steel beams (spacing 4 m) and a small longitudinal beam, Fig. 6 c shown the partial diagram of the main girder.

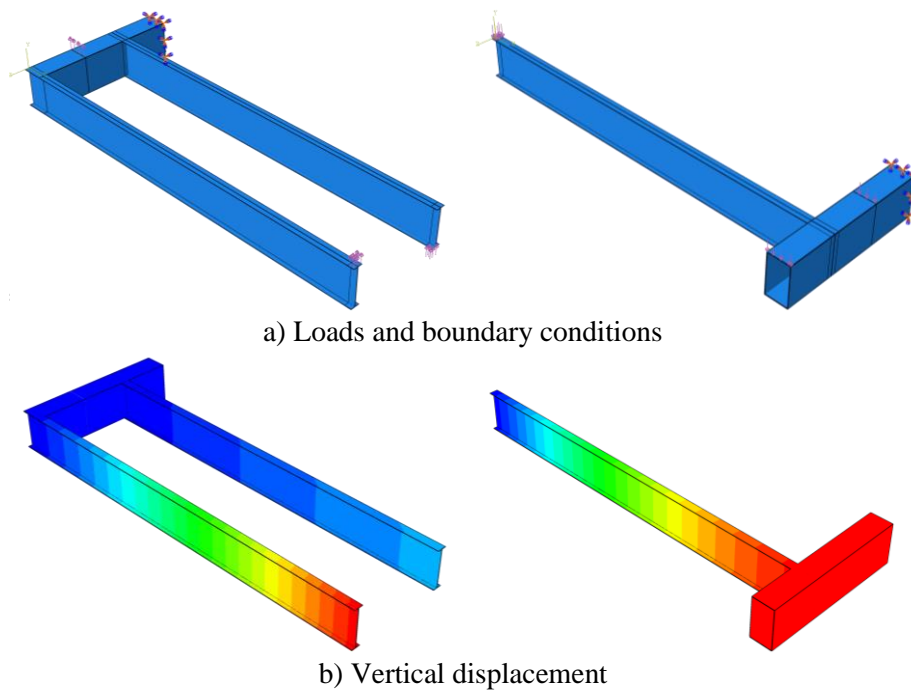


Figure 5: Finite element models of local space.

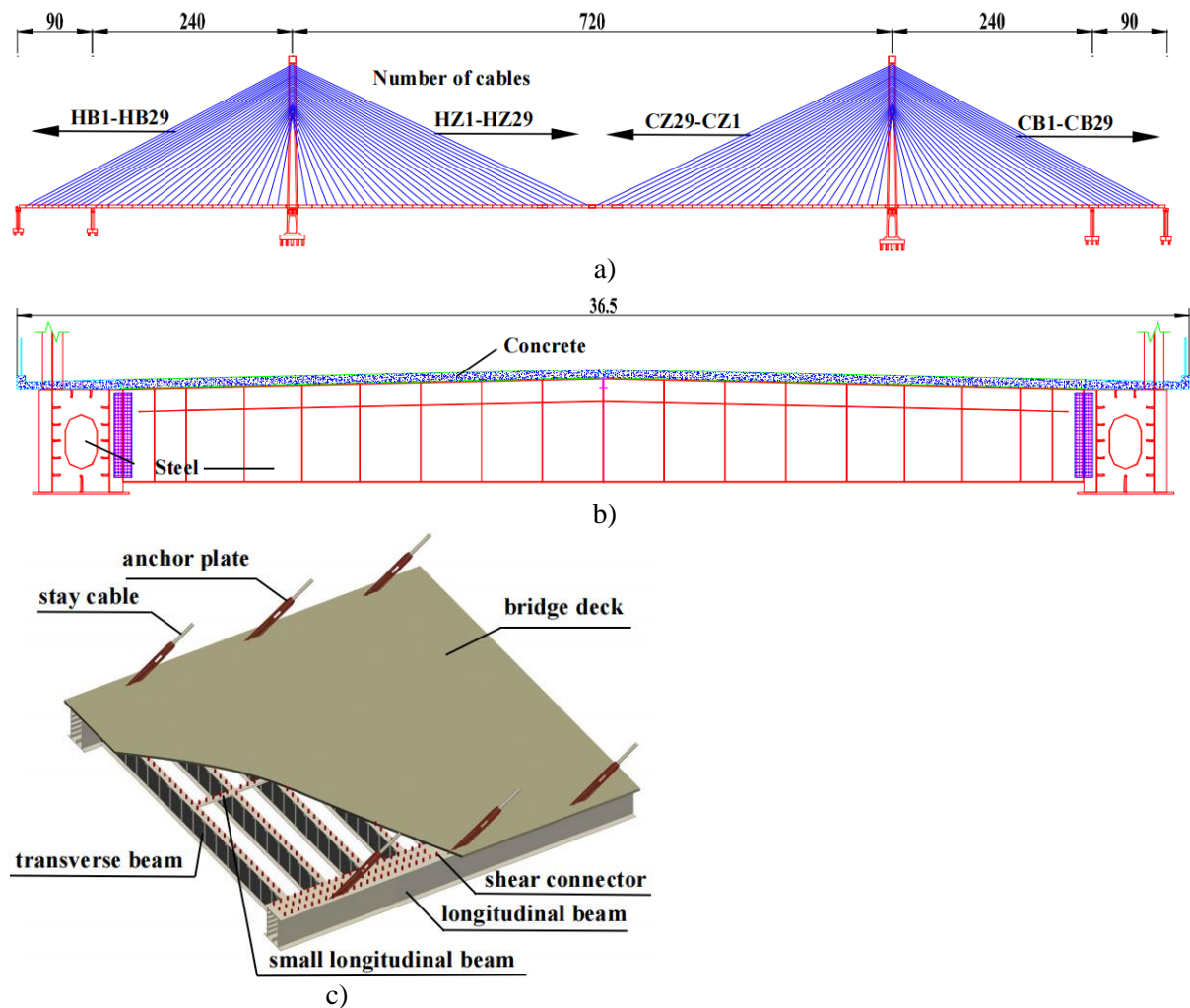


Figure 6: A Yangtze River Bridge: a) Elevation of the main bridge (units: m); b) Standard cross-section of the composite girder (units: m); c) Local schematic diagram of the main girder.



### 4.2 Theoretical analysis results

Based on the theoretical analysis in Section 3.1 and substituting the relevant parameters of the main girder of the cable-stayed bridge above, the values of  $X_1$ ,  $X_2$  and  $X_3$  corresponding to different values of  $\theta_1$  and  $\theta_2$  can be obtained. Considering the completely symmetrical frame structure of the twin-box girder, the torsion angle generated owing to installation errors is generally within  $\pm 0.3^\circ$ . The value of  $\theta_1$  is set within the range of  $0^\circ$ - $0.3^\circ$ , and the value of  $\theta_2$  is set within the range of  $-0.3^\circ$ - $0.3^\circ$ . Fig. 7 depicts the corresponding values of  $X_1$ ,  $X_2$  and  $X_3$ .

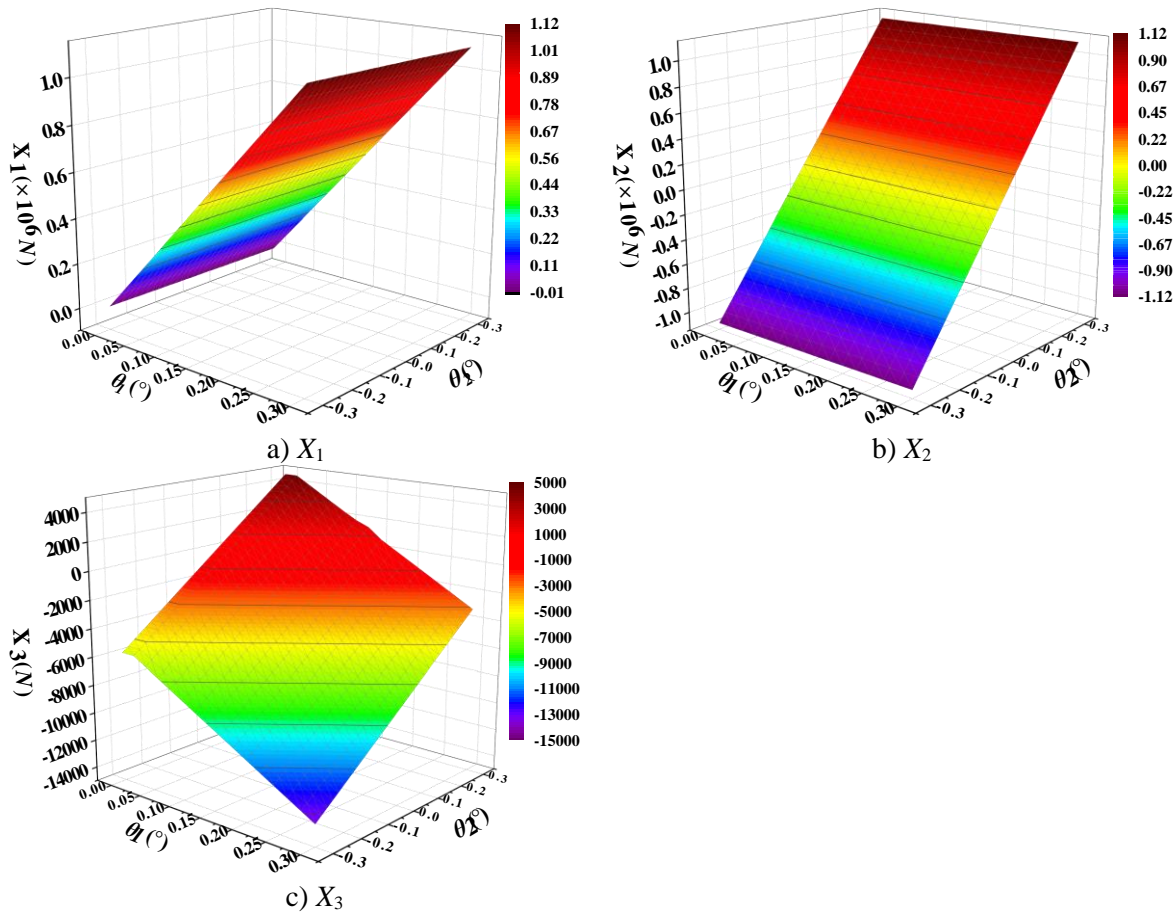


Figure 7: Values of  $X_1$ ,  $X_2$  and  $X_3$  corresponding to different values of  $\theta_1$  ( $0$ - $0.3^\circ$ ) and  $\theta_2$  ( $-0.3^\circ$ - $0.3^\circ$ ).

### 4.3 Field verification

In the actual construction of a composite girder cable-stayed bridge, the torsion angle of the left steel longitudinal beam of the steel main girder of the #5 segment,  $\theta_1$  was  $2.0^\circ$ , and the torsion angle of the right steel longitudinal beam,  $\theta_2$ , was  $-1.6^\circ$ . The torsion angles were adjusted using a steel transverse beam multipoint jacking adjustment device (Fig. 8). Table I presents the values of  $X_1$ ,  $X_2$  and  $X_3$  obtained from theoretical calculation, numerical analysis and field measurement based on the theoretical calculation in Section 3.1 and the ABAQUS finite element analysis in Section 3.2. The theoretical and numerical solutions are close to the measured values, indicating the validity of the theoretical and numerical calculations. Through the jacking measure, the errors caused by the torsion angle of the steel longitudinal beams of the composite twin-box girder were nearly eliminated and met the requirements of precise alignment of the steel beam. In addition, the bolt holes of the steel longitudinal and transverse beams were quickly aligned with the bolt holes of the splice plate, so the steel transverse beams were installed smoothly.

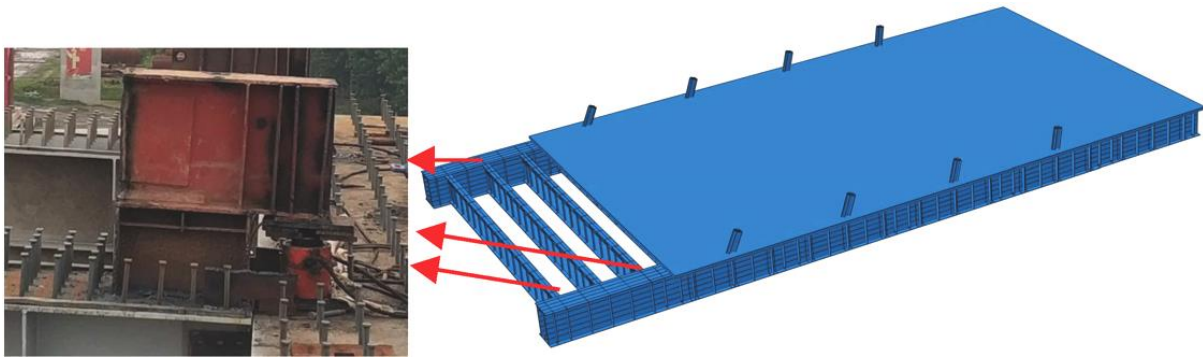


Figure 8: Position of the jacking device.

Table I: The jacking forces corresponding to  $\theta_1 = 2.0^\circ$  and  $\theta_2 = -1.6^\circ$  under different calculation methods.

Calculation method	Jacking force (kN)		
	$X_1$	$X_2$	$X_3$
Analytical solution	744	-577	8
Numerical solution	727	-563	7
Measured value	756	-593	7

## 5. CONCLUSION

This study examined the torsion of the main girder using theoretical calculations, numerical simulations and field measurements. The aim was to address the misalignment issue that arises from the inability to connect steel longitudinal beams and steel transverse beams via the splice plate. This problem was due to the torsion of the steel longitudinal beams, which was caused by installation errors of the main girder in the composite twin-box girder cable-stayed bridge. Finally, the following conclusions could be obtained:

(1) The constrained torsion differential equation for steel longitudinal beams is established based on the constrained torsion calculation theory for closed thin-walled members, and the general solution of the differential equation is solved using the initial parameter method. On this basis, the theoretical calculation formula for the jacking forces in the jacking adjustment of transverse steel beams is deduced.

(2) A torsion correction method through multipoint jacking adjustment of steel transverse beams is proposed based on theoretical calculations and ABAQUS finite element analysis. The field measurements show that the torsion correction method proposed in this study has a good implementation effect and can quickly align the bolt holes of the steel longitudinal and transverse beams with the bolt holes of the splice plate. Consequently, the steel transverse beams can be installed smoothly, providing a reference for correcting the main girder torsion of other composite girder cable-stayed bridges.

(3) The values of the jacking forces  $X_1$ ,  $X_2$  and  $X_3$  obtained through theoretical calculation and numerical simulation are very close to the measured values. This result indicates that the theoretical analysis and modelling methods have good accuracy.

In this study, theoretical analysis, finite element numerical analysis and field measurements are combined to analyse the problem of main girder torsion in a composite twin-box girder cable-stayed bridge during the construction stage. The torsion correction method through multipoint jacking adjustment of transverse steel beams proposed in this study has a certain reference value for the future construction of main girders of composite girder cable-stayed bridges. The research object is limited to a twin-box composite girder. Thus, the proposed torsion correction method is not necessarily suitable for other types of

composite girders, such as twin I-shaped composite steel girders, PK box composite girders and closed box composite girders. Therefore, future research can study the main girder installation process of additional types of composite girder cable-stayed bridges to deepen the understanding of the main girder torsion problem and to develop additional convenient torsion correction methods.

## **ACKNOWLEDGEMENT**

This study was supported by the National Natural Science Foundation of China (Grant No. 51878073, No. 52278143 and No. 52278141) and the Research Foundation of Education Department of Hunan Province (Grant No. 19A208). The authors express their great appreciation and sincere gratitude.

## **REFERENCES**

- [1] Cui, B.; Wu, H. L.; Zhao, C. H.; Liu, J. P.; Guo, Z. M. (2023). Steel-concrete composite cable-stayed bridge-main bridge of the Jiangxinzhou Yangtze river bridge at Nanjing, *Structural Engineering International*, Vol. 33, No. 1, 107-114, doi:[10.1080/10168664.2021.1999191](https://doi.org/10.1080/10168664.2021.1999191)
- [2] Yan, L.; Ren, L.; He, X. H.; Li, Y.; Du, B.; Zhong, R. L. (2020). Experimental study of buffeting control of Pingtang bridge during construction, *Journal of Bridge Engineering*, Vol. 25, No. 8, Paper 05020004, 14 pages, doi:[10.1061/\(ASCE\)BE.1943-5592.0001577](https://doi.org/10.1061/(ASCE)BE.1943-5592.0001577)
- [3] Cao, M. M.; Han, Y. Y.; Wei, L. Y. (2019). Precise matching technique for segmental lifting and erection of wide PK composite girder of long-span cable-stayed bridge, *Bridge Construction*, Vol. 49, No. 6, 54-59
- [4] Xu, J. Y.; Yan, Q. S.; Wang, W. J.; Han, D. J. (2007). Section deformation of flat hollow steel box girder of cable-stayed bridge during cantilever erection, *Journal of South China University of Technology (Natural Science Edition)*, Vol. 2007, No. 3, 127-131
- [5] Sun, L. P.; Yong, Y. J.; Yang, Y. H.; Cai, Y. B. (2018). Research on key problems of matching technology in cantilever erection of navigation opening bridge of Taizhou Bay cross-sea bridge, *Bridge Construction*, Vol. 48, No. 6, 116-121
- [6] Wang, L. B.; Liu, P.; Li, Y.; He, S. H. (2016). Research on matching technology in cantilever erection for wide steel box girder of cable-stayed bridge, *China Journal of Highway and Transport*, Vol. 29, No. 12, 102-141
- [7] Cai, Y. B.; Sun, L. P.; Yang, Y. H.; Wang, X. (2022). Study of main girder deformation and load bearing behavior of cable-stayed bridge during cantilever assembly of steel box-concrete composite girder, *World Bridge*, Vol. 50, No. 6, 86-93
- [8] Jiang, Z. G.; Tang, J. R. (2023). Study of precise girder segment matching techniques for north main bridge of Qidu bridge in Wenzhou, *World Bridge*, Vol. 51, No. S1, 104-109
- [9] Du, S.; You, X. P.; Peng, C. M. (2015). Technology of precasting and installing for integral segment in composite girder cable-stayed bridge, *Advanced Materials Research*, Vol. 1065-1069, 976-983, doi:[10.4028/www.scientific.net/AMR.1065-1069.976](https://doi.org/10.4028/www.scientific.net/AMR.1065-1069.976)
- [10] Morgenthal, G.; Sham, R.; West, B. (2010). Engineering the tower and main span construction of stonecutters bridge, *Journal of Bridge Engineering*, Vol. 15, No. 2, 144-152, doi:[10.1061/\(ASCE\)BE.1943-5592.0000042](https://doi.org/10.1061/(ASCE)BE.1943-5592.0000042)
- [11] Deng, X. G.; Liu, M. Y. (2015). Nonlinear stability analysis of a composite girder cable-stayed bridge with three pylons during construction, *Mathematical Problems in Engineering*, Vol. 2015, Paper 978514, 9 pages, doi:[10.1155/2015/978514](https://doi.org/10.1155/2015/978514)
- [12] Kaern, J. C.; Hansen, J. E. (2017). Queensferry crossing cable-stayed composite bridge, *Ce/papers*, Vol. 1, No. 2-3, 4143-4152, doi:[10.1002/cepa.471](https://doi.org/10.1002/cepa.471)
- [13] Wang, C.-S.; Zhang, W.-T.; Li, H.-T.; Zhai, X.-L.; Xin, Y.-F. (2022). Shear lag effect of twin I-shaped composite girders in cable-stayed bridges, creep and shrinkage effects in steel-concrete composite beams, *Thin-Walled Structures*, Vol. 180, Paper 109822, 14 pages, doi:[10.1016/J.TWS.2022.109822](https://doi.org/10.1016/J.TWS.2022.109822)

- [14] Wang, C.-S.; Zhang, W.-T.; Yang, M.-Y. (2023). Shear lag effect of composite girders in cable-stayed bridges under dead loads, *Engineering Structures*, Vol. 281, Paper 115752, 18 pages, doi:[10.1016/j.engstruct.2023.115752](https://doi.org/10.1016/j.engstruct.2023.115752)
- [15] She, Q. C.; Chen, C. S.; Yan, D. H.; Wu, L. M.; Huang, G. (2022). Shear lag effect study of a composite girder cable-stayed bridge during construction, *International Journal of Simulation Modelling*, Vol. 21, No. 4, 555-566, doi:[10.2507/IJSIMM21-4-615](https://doi.org/10.2507/IJSIMM21-4-615)
- [16] Zhao, C. H.; Guan, W. B.; Deng, K. L.; Yu, D. A.; Hong, Y. (2023). Precise matching technology for segment hoisting of cable-stayed bridge bilateral box lightweight composite girder, *Construction Technology*, Vol. 52, No. 2, 33-36
- [17] Atmaca, B.; Ates, S. (2012). Construction stage analysis of three-dimensional cable-stayed bridges, *Steel and Composite Structures*, Vol. 12, No. 5, 413-426, doi:[10.12989/scs.2012.12.5.413](https://doi.org/10.12989/scs.2012.12.5.413)
- [18] Giaccu, G. F.; Briseghella, B.; Fenu, L. (2022). Numerical simulation and simplified calculation of the effective slab width for composite cable-stayed bridges, *Structures*, Vol. 39, 512-526, doi:[10.1016/j.istruc.2022.03.034](https://doi.org/10.1016/j.istruc.2022.03.034)
- [19] Szurgott, P.; Bernacki, P. (2020). Modelling of steel-concrete bridges subjected to a moving high-speed train, *International Journal of Simulation Modelling*, Vol. 19, No. 1, 29-40, doi:[10.2507/IJSIMM19-1-499](https://doi.org/10.2507/IJSIMM19-1-499)
- [20] Gao, R. Y.; Xin, Q.; Hu, X. Q.; Liang, C. Y. (2022). Residual performance analysis of bridge structure considering heavy load effect, *Dyna*, Vol. 97, No. 2, 156-161, doi:[10.6036/10440](https://doi.org/10.6036/10440)
- [21] Gara, F.; Leoni, G.; Dezi, L. (2009). A beam finite element including shear lag effect for the time-dependent analysis of steel-concrete composite decks, *Engineering Structures*, Vol. 31, No. 8, 1888-1902, doi:[10.1016/j.engstruct.2009.03.017](https://doi.org/10.1016/j.engstruct.2009.03.017)
- [22] Gara, F.; Ranzi, G.; Leoni, G. (2010). Short- and long-term analytical solutions for composite beams with partial interaction and shear-lag effects, *International Journal of Steel Structures*, Vol. 10, No. 4, 359-372, doi:[10.1007/bf03215844](https://doi.org/10.1007/bf03215844)